



HAL
open science

Buckling of tension-loaded thin-walled composite plates with cut-outs

T. Kremer, H. Schürmann

► **To cite this version:**

T. Kremer, H. Schürmann. Buckling of tension-loaded thin-walled composite plates with cut-outs. *Composites Science and Technology*, 2009, 68 (1), pp.90. 10.1016/j.compscitech.2007.05.035 . hal-00524476

HAL Id: hal-00524476

<https://hal.science/hal-00524476>

Submitted on 8 Oct 2010

HAL is a multi-disciplinary open access archive for the deposit and dissemination of scientific research documents, whether they are published or not. The documents may come from teaching and research institutions in France or abroad, or from public or private research centers.

L'archive ouverte pluridisciplinaire **HAL**, est destinée au dépôt et à la diffusion de documents scientifiques de niveau recherche, publiés ou non, émanant des établissements d'enseignement et de recherche français ou étrangers, des laboratoires publics ou privés.

Accepted Manuscript

Buckling of tension-loaded thin-walled composite plates with cut-outs

T. Kremer, H. Schürmann

PII: S0266-3538(07)00235-7
DOI: [10.1016/j.compscitech.2007.05.035](https://doi.org/10.1016/j.compscitech.2007.05.035)
Reference: CSTE 3726

To appear in: *Composites Science and Technology*

Received Date: 20 March 2007
Revised Date: 4 May 2007
Accepted Date: 20 May 2007



Please cite this article as: Kremer, T., Schürmann, H., Buckling of tension-loaded thin-walled composite plates with cut-outs, *Composites Science and Technology* (2007), doi: [10.1016/j.compscitech.2007.05.035](https://doi.org/10.1016/j.compscitech.2007.05.035)

This is a PDF file of an unedited manuscript that has been accepted for publication. As a service to our customers we are providing this early version of the manuscript. The manuscript will undergo copyediting, typesetting, and review of the resulting proof before it is published in its final form. Please note that during the production process errors may be discovered which could affect the content, and all legal disclaimers that apply to the journal pertain.

Buckling of tension-loaded thin-walled composite plates with cut-outs

T. Kremer^{a,*},

H. Schürmann^a

^a*Darmstadt University of Technology, Department of Lightweight Design and
Construction, Petersenstraße 30, 64287 Darmstadt, Germany*

Abstract

Plane plates subjected to tensile loads are usually not considered to fail due to buckling. However if a plate contains a cut-out, regions of compressive stresses arise under a uniaxial tensile load. In thin-walled orthotropic composite plates these compressive stresses may cause local buckling.

In general the stress concentration factors of cut-outs are very high, thus the buckling limits will not be exceeded before fracture. However cut-outs, optimised by a shape optimisation method, run risk to initiate buckling before exceeding the fracture load because the stress concentration factors for these cut-outs are very low.

In this paper the influence of the shape of optimised cut-outs on the buckling behaviour is investigated. Besides the critical load the under-critical and post-critical behaviour of geometrical imperfect orthotropic composite plates is analysed. Methods that prevent local buckling under tensile stresses are discussed in order to provide the full advantage of optimised cut-outs.

Key words:

B. Buckling, B. Notch

PACS: 81.05.Qk

1 Introduction

Buckling under nominal compressive loads is well known. Even the influence of cut-outs on the buckling load is widely investigated (1) but only a few considerations are made on buckling under a nominal tension load. Nevertheless buckling under tensile loads can be found in various geometries, even in a pulled flat strip (2). Plates disturbed by cut-outs are notably affected since holes create an inhomogeneous stress field with high tensile and compressive stresses. The presence of compressive stresses always indicates a possible buckling problem.

In the past only a few papers dealt with buckling at cut-outs under a global tensile load. Since *Cherepanov* (3) in 1963 described the problem for the first time, it took a long period until further results had been published. A main focus had been put on isotropic materials and only a few papers took the orthotropic behaviour of composite plates into account (4; 5). To the authors best knowledge even for the case of a plate containing a circular hole no analytic expression for the buckling load with respect to the orthotropic elasticity exists.

* Corresponding author. Address: TU Darmstadt, Fachgebiet Konstruktiver Leichtbau und Bauweisen, Petersenstraße 30, 64287 Darmstadt, Germany. Tel. +49 6151 166532, Fax +49 6151 163260

Email addresses: tobias.kremer@klub.tu-darmstadt.de (T. Kremer),
helmut.schuermann@klub.tu-darmstadt.de (H. Schürmann).

The buckling load of composite plates is dominated by the local bending stiffness which depends on the spatial direction, the stacking sequence and the fibre orientation. Besides the bending stiffness the in-plane parameters of elasticity influence the critical load. With the aid of the finite element method (FEM) one is able to estimate buckling coefficients with respect to the orthotropic properties of the plate, like done in (4; 6), but no analytical solution has been found so far. *Larsson* notes that even the influence of the Poisson's ratio and the shear modulus on the buckling load can hardly be described.

While this section deals with the behaviour of isotropic plates as an introduction, sections 2 to 4 take orthotropic composite plates into account.

1.1 Fracture load and critical load

The *fracture load* (index: fr) is the maximum load a plate can carry without generating a crack under the assumption that no out of plane deflection is allowed. Therefore the fracture load is determined by the stress distribution and the strength of the material. Failure of composite plates is differed in fibre failure and inter-fibre failure.

Considering the stability problem, the eigenvalue of the linear buckling problem is equal to the *critical load* (index: cr). Thus the critical load is the maximum load a plate can carry without an out of plane deflection, ignoring whether the material's strength is exceeded or not. Only terms of stiffness and the stress distribution affect the critical load.

For real structural applications the minor of both loads determines the maximum applicable load. Especially since modern shape optimisation methods are able to rise the fracture load of structures disturbed by cut-outs the buckling load is of major interest in a design process. However, by shape optimisation the absolute value of compressive stresses can – in many cases – not be reduced in the same way tensile stresses are minimized. This leads to an increasing relevance of the stability problem, because tensile stresses are decreasing and compressive stresses remain on their level.

1.2 Geometrical imperfections

Another aspect, which makes it necessary to consider buckling of plates under tensile loads, is that real structures always include geometrical imperfections. Imperfections may arise from the manufacturing process or an imperfect bearing. These imperfections cause out of plane deflections at undercritical loads. Thus a structure can only reach its fracture load if the critical load is significant higher.

Since the buckling and post-buckling behaviour of isotropic plates with circular holes is quite well understood, this case is used to make the buckling mechanism clear.

1.3 Buckling and post-buckling mechanism in isotropic plates

1.3.1 Model description

A thin-walled aluminum plate with a central circular hole is chosen as an example to explain the buckling mechanism. The thickness of the plate is $t = 0.01$ mm, so the thickness corresponds to a standard aluminum foil. Table 1 summarises the parameters introduced in figure 1. The parameters of the present plate are identical with the experimental setup of *Gilabert* (7). This makes the numerical results, obtained in this paper, comparable to *Gilabert's* experimental results. The plate is placed in the xy -plane, as shown in figure 1, and discretised in order to solve the problem with a standard finite element program. The whole structure was discretized by approximately 6000 and the cut-out by 160 linear shell elements. The elements are based on the equations of *Kirchhoff's* theory. In the case of layered materials the classical lamination theory (CLT) is used to obtain the layer-wise stresses. The basic theory can be found in (8), for example.

The critical load and the corresponding buckling mode were obtained by a linear eigenvalue analysis using the *Lanczos* method. After this analysis a general nonlinear static procedure was used to obtain the stress distribution and to perform the post-buckling analysis.

The edges in x -direction are coupled to a rigid bar, the edges in y -direction are free. Setting the edges rigid will ensure that all nodes at the edge perform the same displacement. Thus the tensile load can be applied directly to the bar. Regarding the cross-section of the plate $A = t \cdot W$ the external load F can be transformed to a mean uniaxial stress $\sigma_{x,0} = F/A$ acting in x -direction.

Table 1

Geometric and elastic properties of an aluminum plate containing a central circular hole

Plate width W	300 mm
Hole diameter D	32 mm
Plate thickness t	0.01 mm
Young's modulus E	72000 N/mm ²
Poisson's ratio ν	0.3

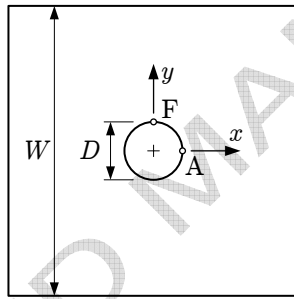


Figure 1. Geometrical parameters of a plate with a central circular hole. "A" denotes the apex and "F" the flank of the hole

1.3.2 Buckling behaviour

Figure 2 shows the result of a static FE-analysis. The minimal principle stress σ_{II} shows a butterflylike pattern with stresses less or equal to zero. These regions will cause local buckling. Because the principal stress state at the cut-out boundary is uniaxial the minimal principle stress corresponds to the σ_y -stress in point A. Therefore the maximum compressive σ_y -stress in the apex is $\sigma_y = -\sigma_{x,0}$. The tangential stress σ_x at point F can be obtained by a stress concentration factor. The K_{tg} -factor for a plate with the present finite width leads to $\sigma_x = K_{tg} \cdot \sigma_{x,0} = 3.04 \cdot \sigma_{x,0}$.

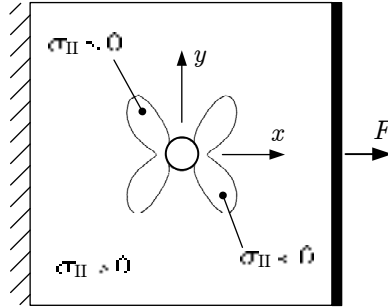


Figure 2. Distribution of the minimal principal stress σ_{II} .

Subsequent to the stress analysis a buckling analysis has been performed. Figure 3 shows the first buckling mode. Regions with high compressive loads are deflected normal to the plate plane in z -direction. Transverse to the load direction the plate remains plane since these regions are dominated by tensile stresses. Although the edges transverse to the load are not clamped, the buckling deflection remains a local effect. This behaviour differs significantly from buckling under a compressive load. Buckling at cut-outs under a global compressive in-plane load always affects major regions of the structure.

Considering the buckling load, one recognizes the very low critical load $F_{cr} = 0.419 \text{ N}$. The corresponding experiments by *Gilabert* showed that at the very beginning of the load-increase first buckling patterns could be observed (7). Since the buckling load depends on the bending stiffness (9) a very small wall thickness, like $t = 0.01 \text{ mm}$ at the current plate, leads to a very low buckling load. Therefore in practice it is possible, that local buckling occurs at significant lower loads than the fracture load.

1.3.3 Post-buckling behaviour

Gilabert's experimental results also showed that a considerable load-increase could be applied, although the critical load had been exceeded.

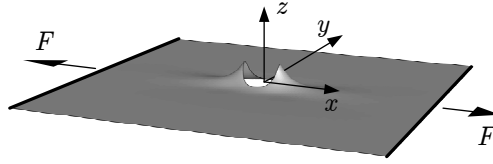


Figure 3. First buckling mode of a plate with circular hole under a tensile load. Corresponding critical load is $F_{cr} = 0.419 \text{ N}$ and accordingly $\sigma_{cr} = 0.14 \text{ N/mm}^2$

By performing a further FEM-analysis the described post-buckling behaviour of the plate was investigated. The post-buckling analysis is based on a geometric imperfect model. Thus a critical load in the sense of a bifurcation load does not longer exists. The term "critical load" always refers to the geometrical perfect model.

As an imperfection the first buckling mode is superimposed to the plate. Other imperfections than the first buckling mode hardly influence the shape of the post-buckling pattern. For this reason the first buckling-mode was chosen as the most critical imperfection. As an amplitude of the imperfection an extremely small value 0.001 mm is chosen. Thus the structure is expected to behave like a quasi-perfect structure. Applying a load to such an imperfect plate will not result in a stability problem but a static bending problem.

Figure 4 shows the plate at a tensile load of $F = 140 \text{ N}$, that is more than 300 times higher than the corresponding critical load. Besides the first buckling mode additional "waves" appear. This behaviour is different from common buckling problems. A column or a plate under a compressive post-critical load will not generate a shape different from the first buckling mode. Additional deflections to the first buckling mode are typical for the post-buckling behaviour of plates with cut-outs under tensile loads. *Gilabert* called these shapes "maltese cross buckling".

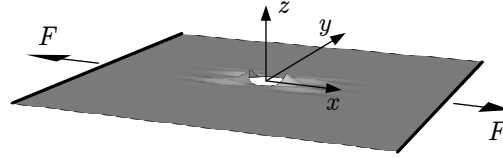


Figure 4. Post-buckling pattern. $F = 140\text{ N}$ and accordingly $\sigma_{x,0} = 46.7\text{ N/mm}^2$.

Scaling factor in z -direction is 50

Considering the total collapse of a structure the loss of global stiffness is of prime importance. Under a constant load a loss of global stiffness leads to large deformations that structures cannot withstand. If a snap-through behaviour can be prevented, structures can be loaded beyond the critical load. Lightweight structures have a strong need for a stable post-buckling behaviour. Since buckling loads in general are very low compared to its corresponding fracture loads, the utilisation factor would be inadmissibly small if post-critical loads would not be accepted.

Figure 5 shows the global in-plane displacement u_x as a function of the normalised load. Since the relation between external load and displacement is linear, no snap-through effect occurs. The plate can be loaded far beyond the critical load without a significant loss of global stiffness. But nevertheless post critical deflections induce high local curvatures.

These curvatures lead to moments and high local bending stresses respectively. The difference between the σ_y -tension on the upper- and underside of the plate is proportional to the additional bending moment. Figure 6 shows these σ_y -stresses. For post critical loads the tension on the upper side turns from a compressive to a tensile stress. At a normalized load of 5 the σ_y -stresses are approximately 4 and 5 times higher than the critical load.

Geometrical imperfections give rise to out-of-plane deflections even for under-

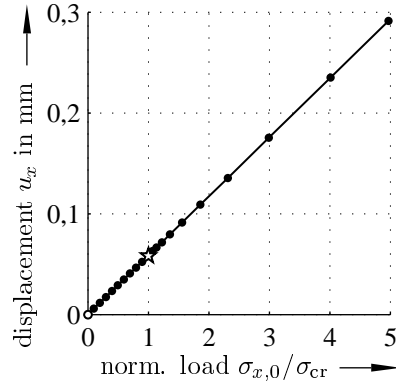


Figure 5. Global displacement of the plate edge in direction of the tensile load. Load is normalised to the critical load. A star marks the critical point.

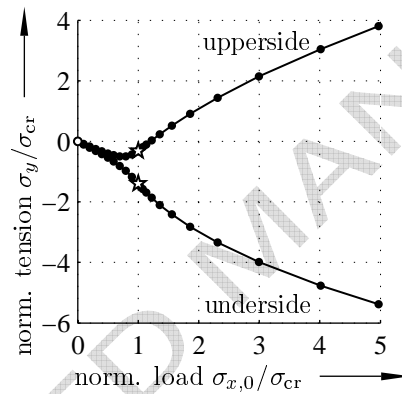


Figure 6. Normalized σ_y -stress at the point of maximum curvature (Point A) at the upper- and underside of the plate. A star marks the critical point.

critical loads. A geometrical perfect structure would not show any under-critical deflections. Therefore a crucial factor is the magnification of out-of-plane deflections which are initialized by geometrical imperfections. The more the deflection increases the higher the local curvature of the plate becomes.

Figure 7 shows the out-of-plane deflection at point A. Displacement is normalised by the plate thickness $t = 0.01\text{mm}$. At a normalised load of 1 the external load is equal to the critical buckling load and the deflection gradient is maximum. Post critical loads still increase the deflection but the gradient is decreasing. Regions with tensile stresses stabilise the deflection and thus there

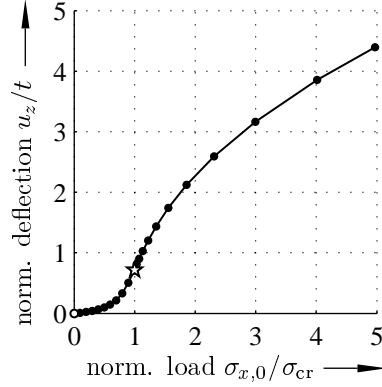


Figure 7. Normalised out of plane deflection at point A. Progressive incline for under-critical loads $\sigma_{x,0}/\sigma_{cr} < 1$. Degressive incline for post-critical loads $\sigma_{x,0}/\sigma_{cr} > 1$. A star marks the critical point.

is no unbounded increase.

1.3.4 Analytical prediction of the buckling load

Buckling of a structure is dominated by a change of the membrane stress state to a bending dominated stress state. Thus there is an obvious dependence of the buckling load on the bending stiffness. As known from *Euler's* buckling stress, the critical load is a linear function of bending stiffness which consists of *Young's* modulus and the wall thickness to the power of three (9; 2; 7).

Besides the bending stiffness the critical load depends on the plate's width W and its hole radius R . To identify the influence of the hole radius, a systematical variation of the relative hole radius R/t was performed. To prevent finite width effects the width W was chosen $W/R > 40$. The following results were computed with the aid of the FEM. *Hooke's* law of the model corresponds to steel $E = 210000 \text{ N/mm}^2$, $\nu = 0.3$.

In figure 8 the gradient of t/σ_{cr} is independent from the radius R . By comput-

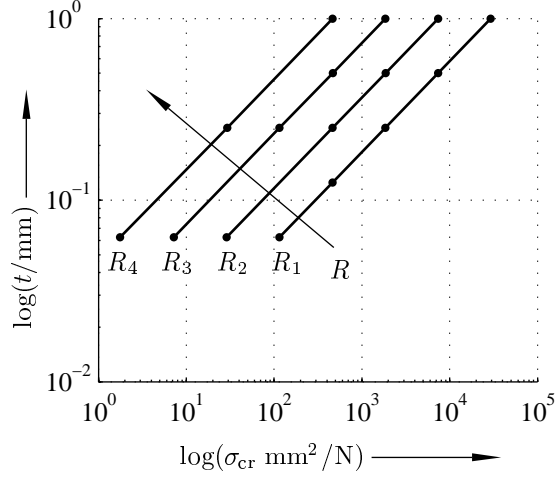


Figure 8. Critical load σ_{cr} as a function of the plate thickness t for different hole radii R for isotropic materials (here: Steel). $R_i = 5, 10, 20, 40$ mm

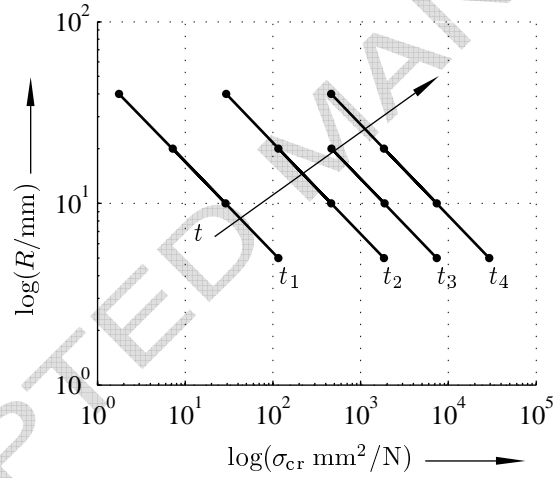


Figure 9. Critical load σ_{cr} as a function of the hole radius R for different plate thickness t for isotropic materials (Steel). $t_i = 0.0625, 0.25, 0.5, 1.0$ mm

ing the gradient in a log-log-domain, one obtains the unknown exponent n of x if the dependence $f(x) = x^n$ is assumed. In the present figure the gradient is $\partial\sigma_{cr}/\partial t = 2$. As mentioned before, the critical load is a function of the bending stiffness. If the critical load is given as a stress, the bending stiffness is divided by the wall thickness t and therefore the critical stress is proportional to t^2 , like found in figure 8.

Figure 9 shows that the gradient, and therefore the exponent of R , does not depend on the plate thickness t . This means that the dependence of t can be expressed without considering the radius R . Computing the gradient one gains -2 which corresponds to $\sigma_{\text{cr}} \propto 1/R^2$.

The buckling stress can now be estimated by the following equation:

$$\sigma_{\text{cr}} = K \cdot E \cdot \frac{t^2}{R^2} \quad (1)$$

E is *Young's* modulus and K a buckling coefficient. Using an isotropic material with an *Poisson's* ratio of $\nu = 0.3$ gives a buckling coefficient of

$$K = 3.55 \quad (2)$$

for an infinite plate. Considering *Euler's* buckling equation of columns in equation (3), for example,

$$\sigma_{\text{cr}} = \pi^2 \cdot E \cdot \frac{1}{\lambda_{\text{cr}}^2} = \frac{\pi^2}{A} \cdot E \cdot \frac{I}{l_{\text{cr}}^2} \quad (3)$$

one can notice an analogy of the structure of equation (1) and *Euler's* buckling equation. The radius R corresponds to effective length l_{cr} which is the geometry term of the buckling equation. $E \cdot I$ is the bending stiffness term in *Euler's* buckling equation which corresponds to the bending stiffness $E \cdot t^2$ expressed in terms of a stress.

2 Optimised cut-outs in layered composites

The CAO.FKV-method is a FEM-based parameter-less shape optimisation method. The boundary of a cut-out is varied by a redesign rule based on an

optimality criterion. As design variables the node coordinates of the discretized FEM model are used. With the help of this method one obtains cut-outs in layered composite materials with a maximum fracture load (10; 11). Since the CAO.FKV-method is based on the physically based fracture criterions by *Puck* (12; 13) the layer-wise *stress exposure*¹ is taken as a measure of the quality of a cut-out shape.

In the present case the maximum stress exposure is taken as a stop condition. If the maximum stress exposure at the complete cut-out is less than 1 – which means that no fracture occurs – the optimization is stopped. The redesign rule is adjusted in a way that regions with a stress exposure less than 1 are not influenced by the algorithm any longer. Without these boundary conditions all cut-outs would degenerate to the global optimum shape for an uniaxial load case: a crack in load-direction. Thus the results of the CAO.FKV-method in the present case depend on the initial cut-out geometry.

The lay-up of the considered CFRP plate is a $[0/90]_S$ cross-ply. The properties of an unidirectional layer which form the cross-ply can be found in table 2. Since no edge effects are included, the stacking sequence does not influence the fracture load, whilst no tension-bending coupling exists. The CAO.FKV-method homogenises the stress exposure for inter-fibre failure in order to raise the fracture load. In the present case the exposure is dominated by stresses σ_2 normal to the fibre direction. Figure 10 shows the distribution of the σ_2 stress around a cut-out in the 90° -layer of the cross-ply. To obtain the optimal

¹ The stress exposure of composite materials is defined in the German VDI-guideline 2014 Part 3

shape, the CAO.FKV-method took approximately 10 iterations.

Table 2

Elastic properties and strength of an unidirectional CFRP layer.

$$E_1 = 139280 \text{ N/mm}^2 \quad R_{\parallel}^+ = 2000 \text{ N/mm}^2$$

$$E_2 = 11672 \text{ N/mm}^2 \quad R_{\parallel}^- = 1650 \text{ N/mm}^2$$

$$G_{21} = 5766 \text{ N/mm}^2 \quad R_{\perp}^+ = 70 \text{ N/mm}^2$$

$$\nu_{21} = 0.26 \quad R_{\perp}^- = 240 \text{ N/mm}^2$$

$$\nu_{12} = 0.022 \quad R_{\perp\parallel} = 105 \text{ N/mm}^2$$

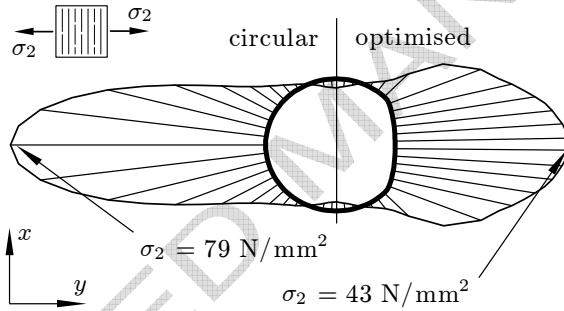


Figure 10. Inter-fibre failure dominating stress σ_2 in the 90° -layer (the layer transverse to the external load) of a cross-ply before and after the shape optimisation. The peak is almost halved.

Figure 11 shows cut-outs with identical fracture loads and cut-out width of $w = 20 \text{ mm}$. The first optimised shape is named *optimised circular* because it is deviated from a circle. The CAO.FKV-method reduced the curvature of the circle until the stress exposure is constant.

The second optimised shape is based on a square, therefore it is called *optimised square*. Besides the curvature of the flank, the edges are softened by the CAO.FKV-method in order to increase the fracture load.

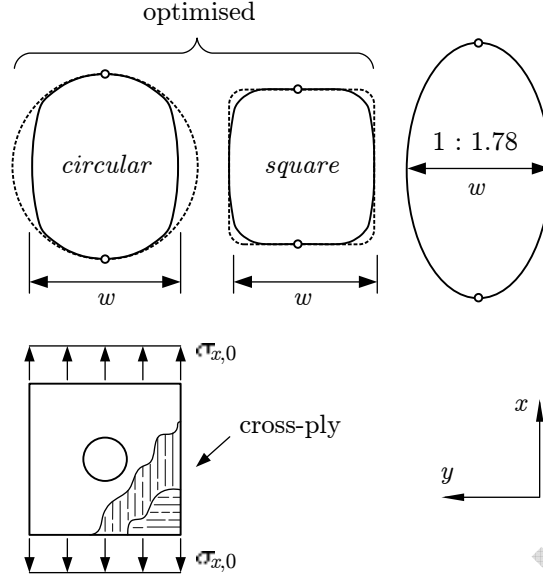


Figure 11. Cut-outs after the shape optimisation. All shapes have the same fracture load and the same width $w = 20$ mm. A small circle indicates the location of the maximum pressure stress σ_y .

The last considered shape is an ellipse. Its aspect ratio is chosen in a way that the fracture load matches the fracture loads of the previous discussed shapes. *Lekhnitskii* showed that compressive stresses at an elliptical cut-out under uniaxial tension does not depend on the aspect ratio (14). The compressive stress at the apex (see point A in figure 1) is given by the following equation.

$$\sigma_{y,A} = -\sigma_0 \sqrt{\frac{E_y}{E_x}} \quad (4)$$

Since the stacking sequence does not influence the modulus E_x and E_y , all cross-ply, with equal layer thickness for 0° - and 90° layers, have a maximum compressive stress of $\sigma_{y,A} = -\sigma_0$. The compressive stresses at the optimised cut-outs are not exactly independent from the cut-out shape. In table 3 the ratio $\sigma_{x,0}/\sigma_{y,A}$ is given. It is found, that the optimised square shape has a significant lower compressive stress.

Table 3

Compressive in-plane stresses at the apex of the cut-outs normalised to the external tension load $\sigma_{x,0}$

cut-out	ratio $\sigma_{x,0}/\sigma_{y,A}$
circular	-1.00
elliptical	-1.00
optimised <i>circular</i>	-0.96
optimised <i>square</i>	-0.76

3 Buckling of layered composites

In the following, two different stacking sequences are examined.

- [0/90/90/0]
- [90/0/0/90]

The first lamina provides a high bending stiffness $D_{11} \cdot t$ in x -direction, thus in the load direction. The second lamina has a high bending stiffness $D_{22} \cdot t$ perpendicular to the load, the y -direction, where t denotes the laminate thickness. Equation (1) showed, that the critical load is expected to be a function of Et^2/R^2 . Because the width of the considered cut-outs is $w = R = 20$ mm, as a free choice, the laminate thickness is chosen $t = 0.25$ mm to provide a suitable t/w -ratio. One has to bear in mind that layups with a greater laminate thickness and at the same time a wider cut-out width are mechanical equivalent as long as they have the same t/w -ratio.

Since the buckling mode is dominated by the curvature κ_y (see figure 3), the high bending stiffness $D_{22} \cdot t$ of a [90/0/0/90] lamina is expected to give higher critical loads. Table 4 lists the critical loads and the corresponding fracture loads for a linear static analysis, neglecting pre-buckling deformations in the static analysis. Ratios σ_{cr}/σ_{fr} smaller than one show that buckling occurs in prior to fracture. At ratios exceeding one, the critical load is higher than the fracture load, thus no buckling occurs because the lamina suffers inter-fibre failure or fibre failure before the buckling load is reached.

Table 4

Critical load σ_{cr} and corresponding tension load at fracture σ_{fr} for different cut-outs and stacking sequences. CFK $t = 0.25$ mm, $w = 20$ mm

stacking sequence	cut-out	σ_{cr} N/mm ²	σ_{fr} N/mm ²	$\frac{\sigma_{cr}}{\sigma_{fr}}$ –
[0/90/90/0]	circular	89	96	0.93
	elliptical	125	145	0.86
	optimised <i>circular</i>	81	145	0.56
	optimised <i>square</i>	62	145	0.42
[90/0/0/90]	circular	300	96	3.13
	elliptical	445	145	3.07
	optimised <i>circular</i>	270	145	1.86
	optimised <i>square</i>	194	145	1.34

As expected, higher bending stiffness in y -direction leads to a higher critical load. Because fracture is assumed to be independent of the stacking sequence the σ_{cr}/σ_{fr} -ratio increases for a [90/0/0/90] lamina and no buckling is expected.

The presumption, that higher induced compressive stresses cause lower critical loads, does not prove true for cut-outs in composite materials. Tables 3 and 4 show that an elliptical cut-out generates the highest compressive stress – compared to an optimised cut-out – but has the highest critical load. Therefore a so far unconsidered parameter, that has to be determined in the following, influences the buckling load as well.

Taking the critical load into account it can be found out, that a high cut-out curvature, at the point of maximum compressive stress, corresponds with a high critical load. The circular hole and the optimised circular shape have exactly the same curvature $1/R$ and almost the same critical load. At the ellipse the curvature is $3.13/R$ and thus the critical load is less than the critical load for a circular hole. Since the boundary of the optimised square cut-out is straight at the point of maximum compressive stress, the cut-out curvature is zero and thus the critical load least.

Nevertheless the dependency on the cut-out curvature can only be assumed in the present discussed cases. Especially for arbitrary lamina configurations the dependence remains to be proved true.

4 Post-buckling behaviour

Ratios σ_{cr}/σ_{fr} less than 1 should be prevented at all circumstances. Even if the critical load is not exceeded, the magnification of imperfections leads to mentionable local bending stresses. The optimised square shape, in a $[0/90/90/0]$ lamina, buckles at 42% of its fracture load. Even if the fracture load is maximum, the exploitation factor of this setup is very low since the applicable load is constrained by the critical load. A simple permutation of the stacking sequence increases the utilisation significantly (see table 4).

Nevertheless the post-buckling behaviour of a $[0/90/90/0]$ layup is analysed in the following because other influences than the buckling behaviour may also influence the choice of this stacking sequence. No attention is paid to the fracture load of the imperfect model in the post-buckling analysis. The main focus is put on the post-buckling mechanisms at the optimised cut-outs. Since these mechanisms do not depend on the amplitude of the imperfection, the imperfection amplitude is chosen to 0.25 mm which corresponds to the thickness of the plate.

Earlier paragraphs of the present paper showed a significant difference in the buckling load of the optimised circle or a square shapes. Therefore the post-buckling behaviour of both shapes is analysed.

Figure 12 shows the region of maximum buckling curvature and thus maximum bending stress at a cut-out. The 90° -layer can not resist high σ_2 stresses, that may lead to inter-fibre failure.

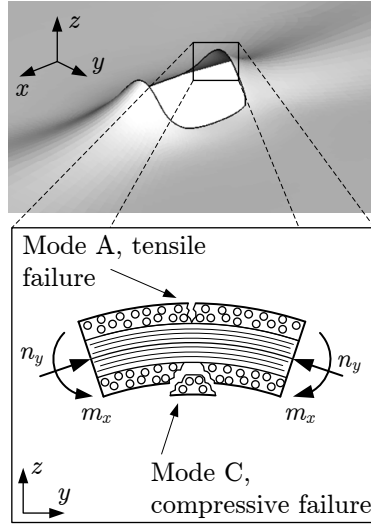


Figure 12. Deflection of an geometric imperfect plate containing a cut-out in the post-buckling analysis. Local curvature causes inter-fibre failure.

Even though the critical load of the optimised *circular* cut-out is 1.3 times higher than the *square* shape (see table 4), no clear difference in the maximum bending moment-flow at these cut-outs could be found. Figure 13 shows the moment-flow $m = M/w$ in x -direction around the *circular* and the *square* shape. The additional bending stresses, caused by the moment, are acting in y -direction and thus rise the σ_2 -load. Since both cut-out shapes are optimised to an identical fracture load and have almost an identical additional bending moment they are expected to fail at the same postcritical load, even though their critical loads differ.

Even if the optimised square shape buckles at an earlier stress state, its final fracture load is not expected to differ significantly from the optimised circular shape. In addition one has to keep in mind, that only a few inter-fibre cracks cause a sudden loss of bending stiffness, see figure 12. A reduced bending stiffness reduces the critical load as well. This mechanism leads, in practice, to lower critical loads than predicted by a numerical analysis.

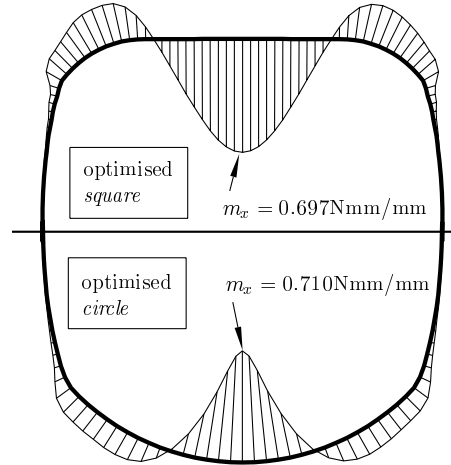


Figure 13. Moment-flow m_x around the optimised cut-outs at the fracture load. Deflection caused by the geometrical imperfect structure.

5 Conclusions

Buckling at cut-outs under a tensile load is not exclusively an academic case. It is relevant for many engineering problems, especially in light weight design. The domination factor is not the bending-stiffness of the plate but the ratio stiffness to cut-out width. *Shimizu et al.* remark that even in design of highway bridges buckling under tensile loads is not negligible (9). In the case of circular holes in isotropic materials the influence of the hole radius on the critical load could be determined. The buckling mechanism of isotropic materials, observed in experiments and numerical analysis, helps to understand buckling of composite materials.

Since shape optimisation methods for FRP give shapes with very high fracture loads, buckling under a tensile load becomes dangerous.

It could be shown that shapes with the same static fracture load differ significantly in their corresponding buckling loads. Besides the cut-out shape the

stacking sequence and the bending stiffness respectively influence the critical load. It was shown, that an improper lay-up results in a undetected stability problem. However an appropriate stacking sequence rises the critical load without influencing the static fracture load.

Post-buckling analysis on geometrical imperfect composite structures were made. Because in practice engineering structures are always superimposed by imperfections, out of plane deflections arise at under-critical loads as well. The analysis showed that the values of the bending moments, resulting from the deflection of the considered shapes, do not significant depend on the critical load.

References

- [1] M. Nemeth, Buckling and postbuckling behaviour of laminated composite plates with a cut-out, in: G. Turvey, I. Marshall (Eds.), *Buckling and Postbuckling of Composite Plates*, 1st Edition, Chapman and Hall, London Glasgow Weinheim, 1995, pp. 260–298.
- [2] N. Friedel, F. Rammertstorfer, F. Fischer, Buckling of stretched stripes, *Computers & Structures* 78 (2000) 185–190.
- [3] G. P. Cherepanov, On the buckling under tension of a membrane containing holes, *Journal of applied mathematics and mechanics* 27 (2) (1963) 275–286.
- [4] P. Larsson, On buckling of orthotropic stretched plates with circular holes, *Composite Structures* 11 (1989) 121–134.
- [5] E. Madenci, A. Barut, Pre- and postbuckling response of curved thin,

- composite panels with cutouts under compression, *International Journal for Numerical Methods in Engineering* 37 (1994) 1499–1510.
- [6] L. R. Kumar, P. Datta, D. Prabhakara, Tension buckling and parametric instability characteristics of doubly curved panels with circular cutout subjected to nonuniform tensile edge loading, *Thin-Walled Structures* 42 (2004) 947–962.
- [7] A. Gilabert, P. Sibillot, D. Sornette, C. Vanneste, D. Maugis, F. Muttin, Buckling instability and pattern around holes or cracks in thin plates under a tensile load, *European Journal of Mechanics, A: Solids* 11 (1) (1992) 65–89.
- [8] A. Leissa, Buckling and postbuckling theory for laminated composite plates, in: G. Turvey, I. Marshall (Eds.), *Buckling and Postbuckling of Composite Plates*, 1st Edition, Chapman and Hall, London Glasgow Weinheim, 1995, pp. 3–29.
- [9] A. Shimizu, S. Yoshida, Buckling of plates with a hole under tension, *Thin-Walled Structures* 12 (1991) 35–49.
- [10] T. Kremer, H. Schürmann, Formoptimierung von geschichteten Faser-Kunststoff-Verbunden mittels eines neu entwickelten CAO.FKV-Verfahrens, *Konstruktion* 11/12 (2006) 63–67.
- [11] T. Kremer, H. Schürmann, Berechnung und Optimierung von Ausschnitten in Faser-Kunststoff-Verbunden, in: *Jahrbuch der Deutschen Gesellschaft für Luft- und Raumfahrt – Lilienthal-Oberth e.V.*, Vol. 1 & 2, DGLR, 2006, pp. 1003–1011.
- [12] A. Puck, H. Schürmann, Failure analysis of frp laminates by means of physically based phenomenological models, in: M. J. Hinton, A. S. Kaddour, P. D. Soden (Eds.), *Failure Criteria in Fiber Reinforced Polymer Composites : The Word-Wide Failure Exercise*, Elsevier Science Ltd,

2004, Ch. 5.6, pp. 832–876.

- [13] A. Puck, Festigkeitsanalyse von Faser-Matrix-Laminaten – Modelle für die Praxis, Carl Hanser Verlag, München Wien, 1996.
- [14] S. G. Lekhnitskii, Anisotropic Plates, 3rd Edition, Gordon and Breach, New York London Paris Montreux Tokyo Melbourne, 1968.

ACCEPTED MANUSCRIPT